

Electronic Supplementary Information

A novel fluorescent peptidyl probe for highly sensitive and selective ratiometric detection of Cd(II) in aqueous and bio-samples via metal ion-mediated self-assembly

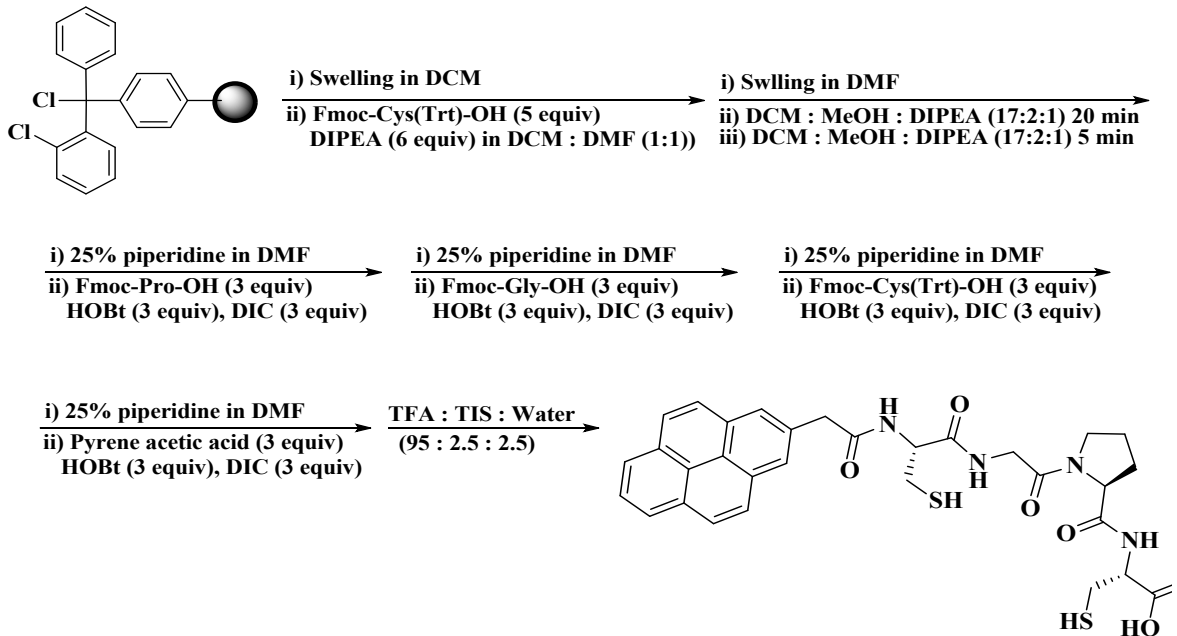
Kwan Ho Jung,^a Semin Oh,^a Joohee Park,^a Yu Jin Park,^a See-Hyoung Park,^{*,b} and Keun-Hyeung Lee^{*,a}

^aCenter for Design and Applications of Molecular Catalysts, Department of Chemistry and Chemical Engineering, Inha University, Incheon, 402-751, South Korea. ^bDepartment of Bio and Chemical Engineering, Hongik University, Sejong 30016, Republic of Korea

E-mail: leekh@inha.ac.kr (K. -H. Lee)

Contents

| | |
|---|-----|
| Scheme S1. Synthesis scheme of 1 | S2 |
| Figure S1. HPLC chromatogram of 1 | S3 |
| Figure S2. ESI-Mass spectrum of 1 | S4 |
| Figure S3. ¹ H NMR of 1 | S5 |
| Figure S4. ¹³ C NMR of 1 | S6 |
| Figure S5. Solvent effect on fluorescence emission spectra of 1 with Cd ²⁺ | S7 |
| Figure S6. Intensity ratio change of 1 with Cd ²⁺ | S8 |
| Figure S7. Emission intensity ratio of 1 induced by various sources of Cd ²⁺ | S9 |
| Figure S8. Interference effect of metal ion on the ratiometric response to Cd ²⁺ | S10 |
| Figure S9. Fluorescent spectra of 1 with Cd ²⁺ in aqueous solutions containing 3% DMF | S11 |
| Figure S10. Job's Plot for 1 with Cd ²⁺ | S12 |
| Figure S11. Non-linear least square fitting of the intensity as a function of concentration of Cd ²⁺ | S13 |
| Figure S12. Reversibility of 1 for Cd ²⁺ | S14 |
| Figure S13. CD Spectra of 1 in the presence and absence of Cd ²⁺ | S15 |
| Figure S14. Linear curve fitting of intensity ratio as a function of Cd ²⁺ in urine samples | S16 |
| Figure S15. Ratiometric response to Cd ²⁺ in ground water samples | S17 |
| Figure S16. Stability performance of 1 | S18 |
| Figure S17. Toxicity study of 1 for cells | S19 |
| Table S1. Comparison of the properties of ratiometric fluorescent probes for Cd(II) | S20 |
| References | S21 |



Scheme S1. Synthetic scheme of **1**.

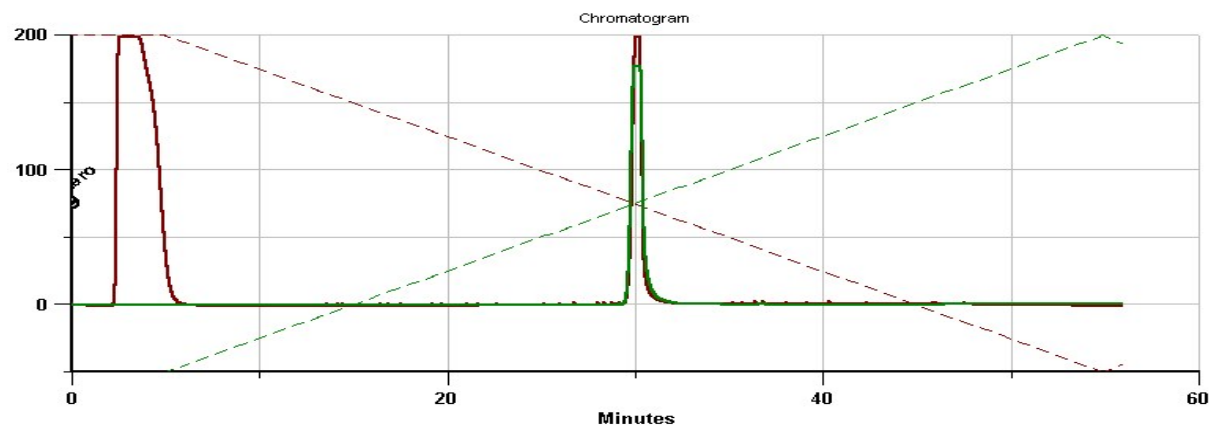


Figure S1. HPLC chromatogram of **1**.

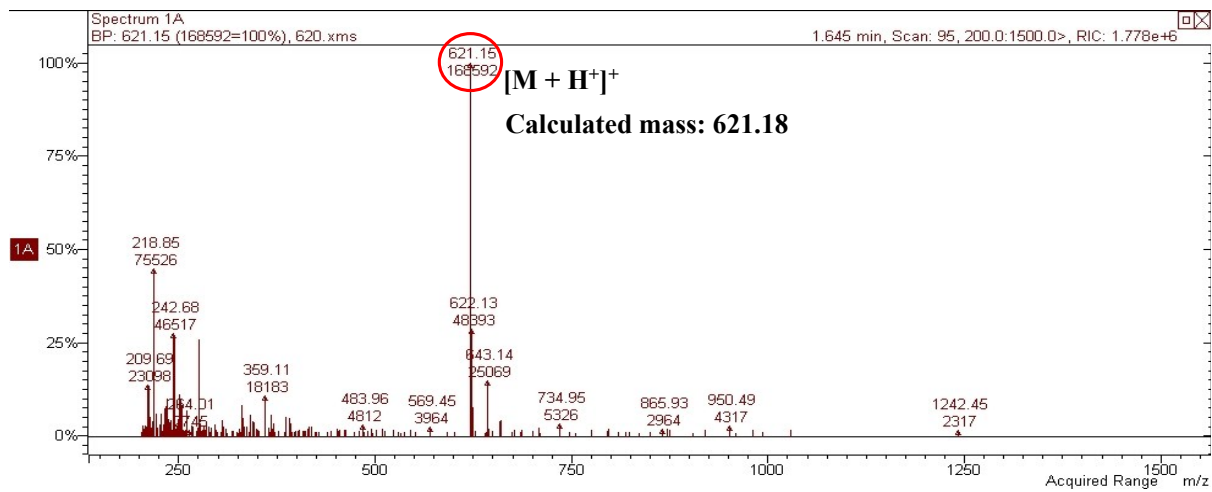


Figure S2. ESI-Mass spectrum of **1**.

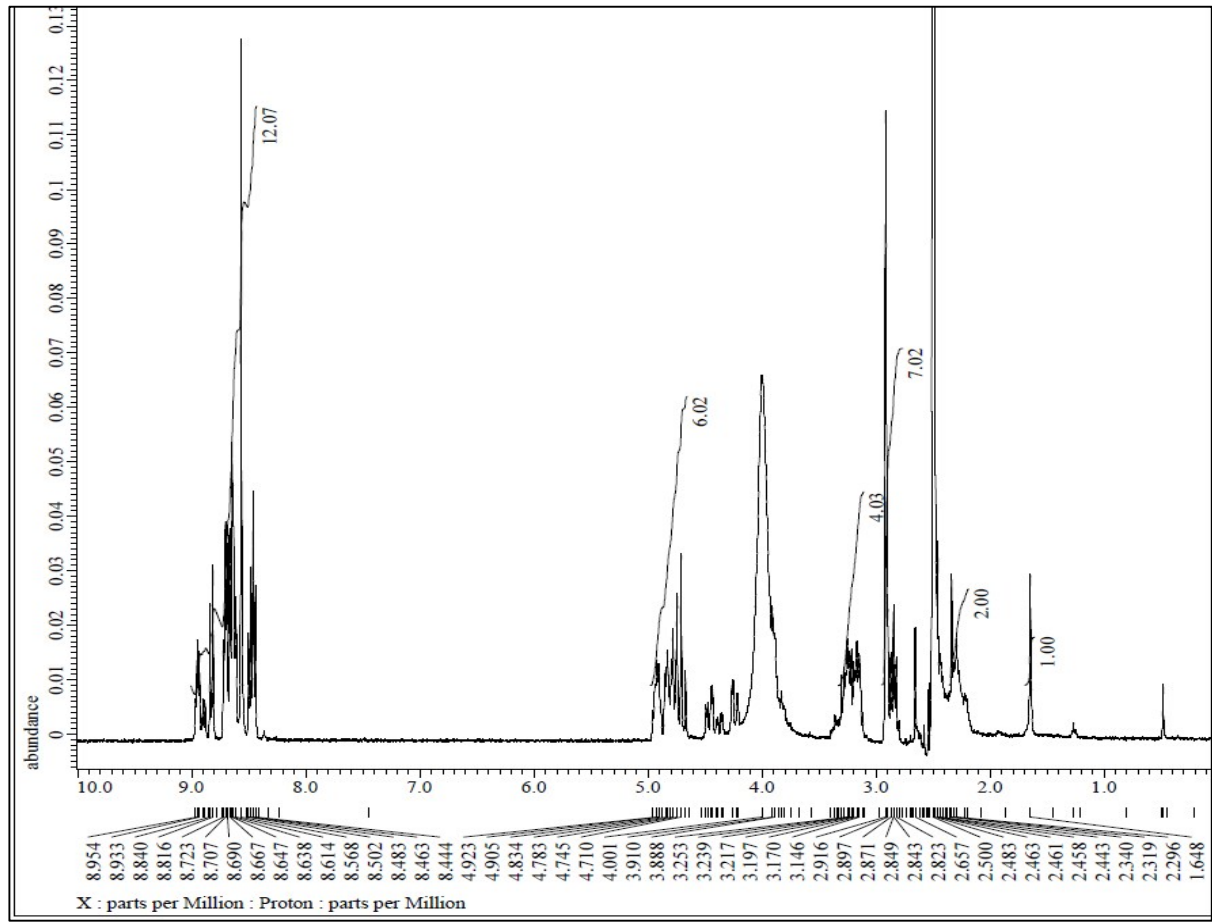


Figure S3. ^1H NMR of **1**.

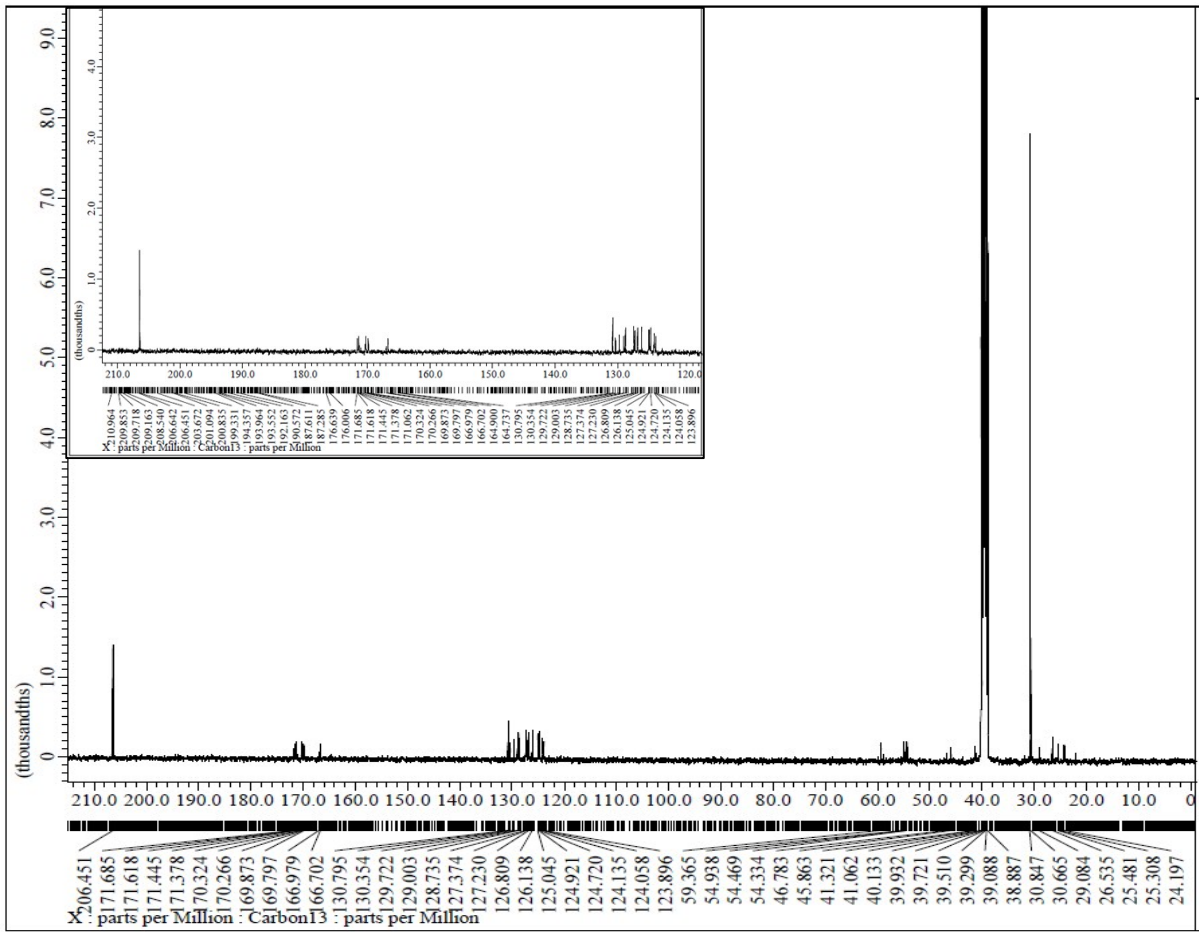


Figure S4. ^{13}C NMR of **1**.

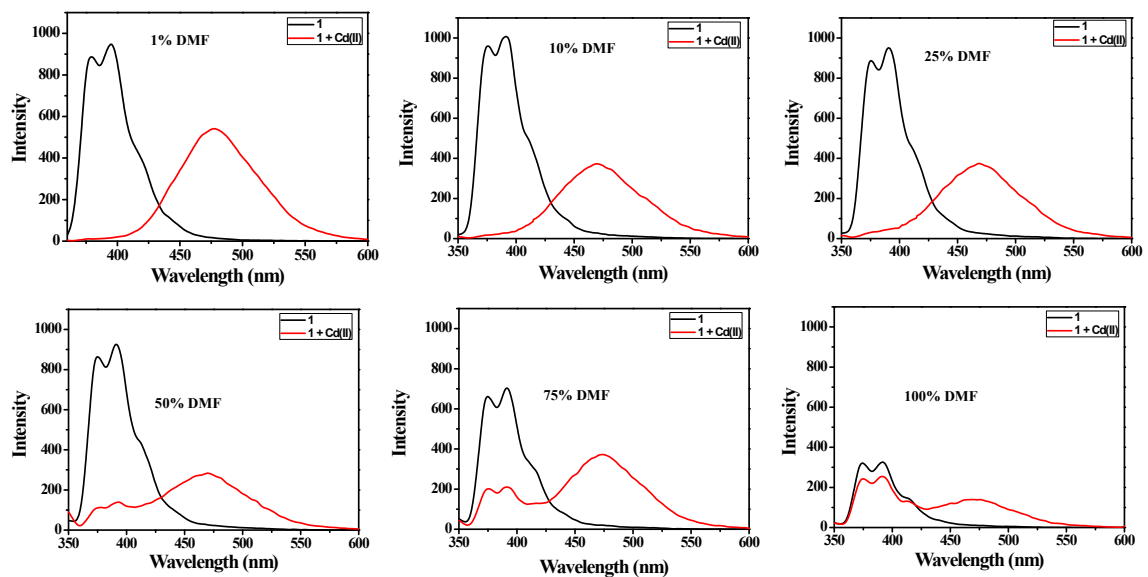


Figure S5. Fluorescence emission spectra of **1** (15 μ M) with Cd^{2+} (15 μM) in aqueous buffered solutions (10 mM, HEPES, pH 7.4) containing various volume of DMF.

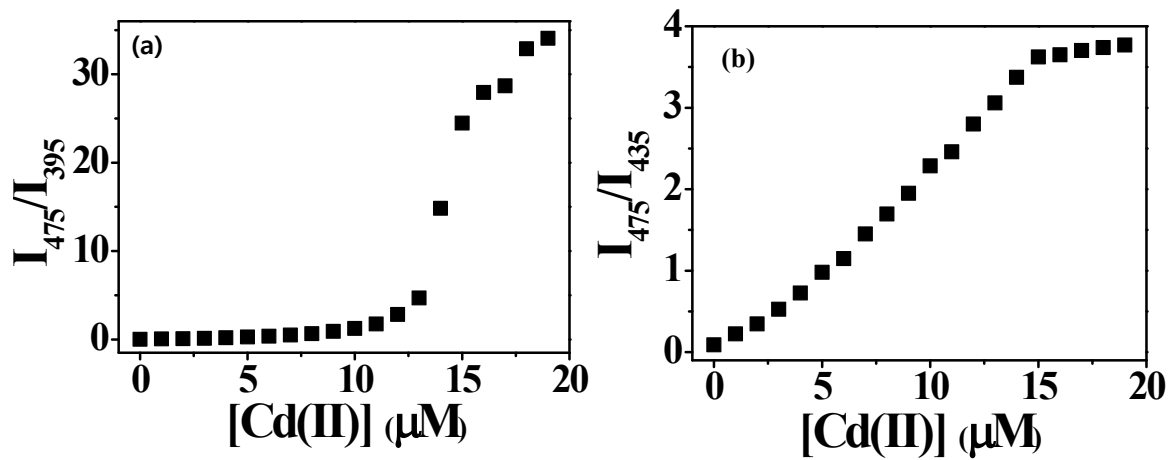


Figure S6. Intensity ratio change (a, I_{475}/I_{395} ; b, I_{475}/I_{435}) of **1** (15 μM) as a function of Cd^{2+} in aqueous buffered solution (10 mM HEPES, pH 7.4) containing 1% DMF ($\lambda_{\text{ex}} = 342 \text{ nm}$).

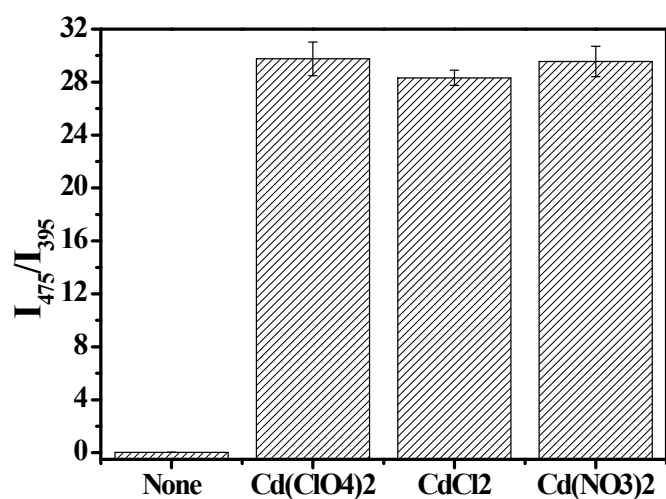


Figure S7. Emission intensity ratio of **1** (10 μ M) induced by various sources of Cd^{2+} (1 equiv) in aqueous buffered solution (10mM HEPES, pH 7.4) containing 1% DMF .

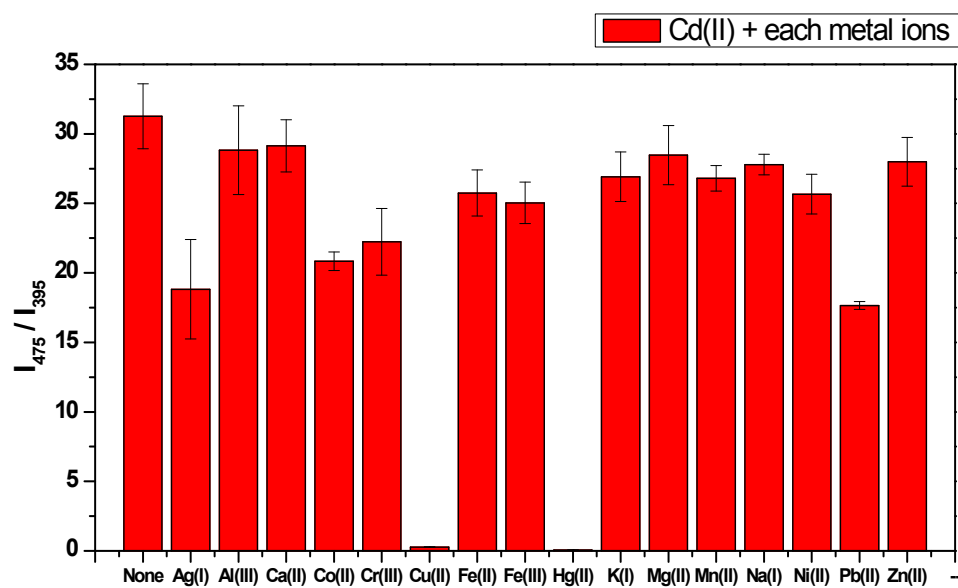


Figure S8. Emission intensity ratio of **1** (15 μ M) in the presence of Cd²⁺ (1 equiv) and various metal ions (5 equiv) in aqueous buffered solution (10mM HEPES, pH 7.4) containing 1% DMF.

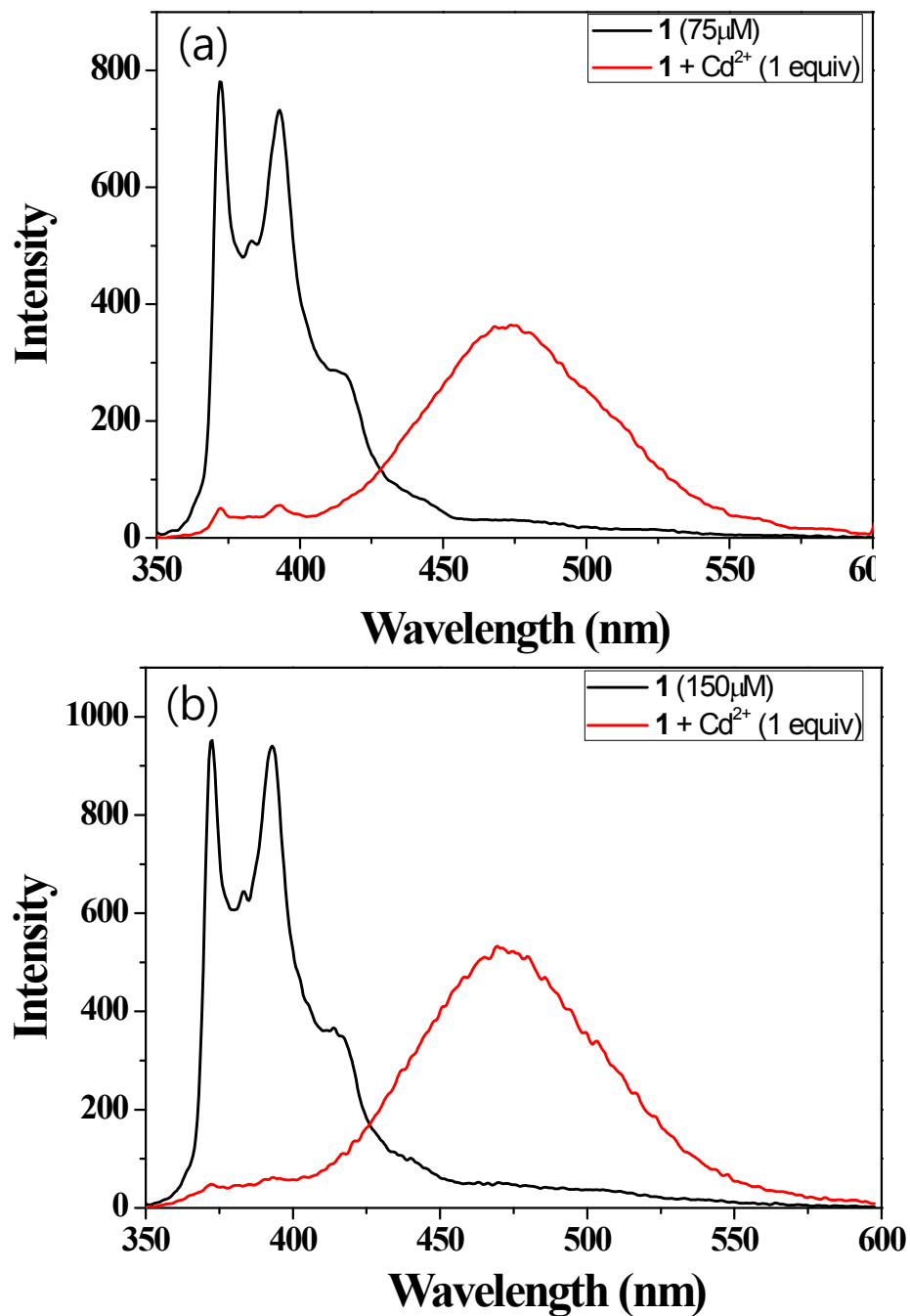


Figure S9. Fluorescence emission spectra of **1** (a; 75 μM , b; 150 μM) in the absence and presence of Cd^{2+} (1 equiv) in aqueous buffered solutions (2 mM, HEPES, pH 7.4) containing 3% DMF ($\lambda_{\text{ex}} = 342 \text{ nm}$).

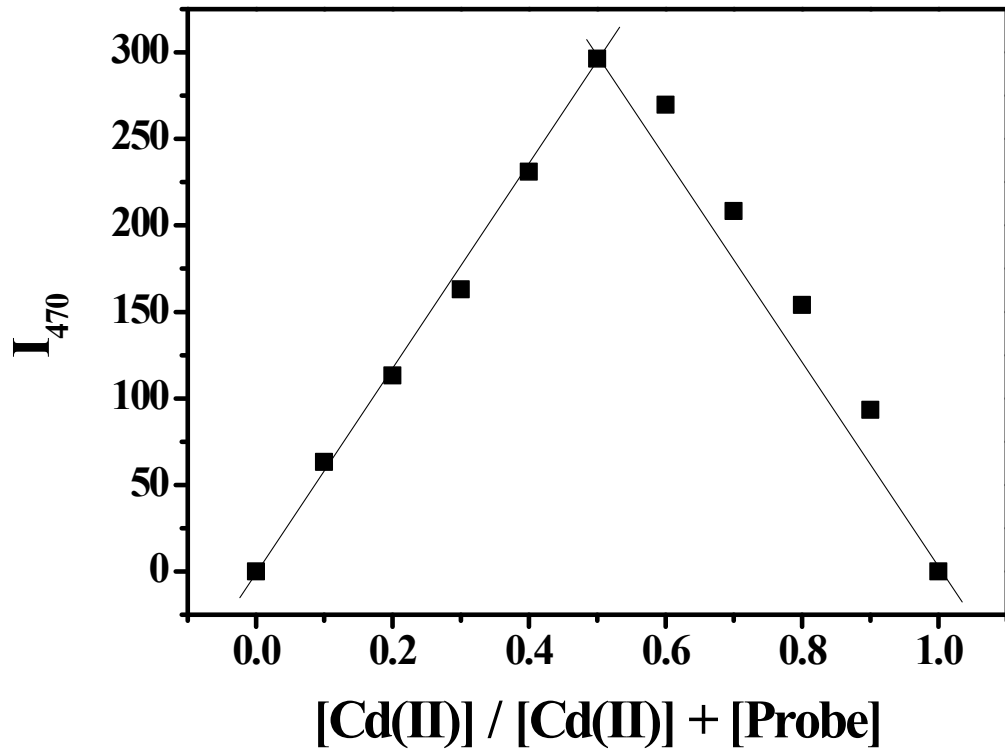


Figure S10. Job's plot for **1** with Cd^{2+} in aqueous buffered solution (10 mM HEPES, pH 7.4) containing 1% DMF; total concentration = 15 μ M, slit 15/12 nm, 1% attenuator ($\lambda_{\text{ex}} = 342$ nm).

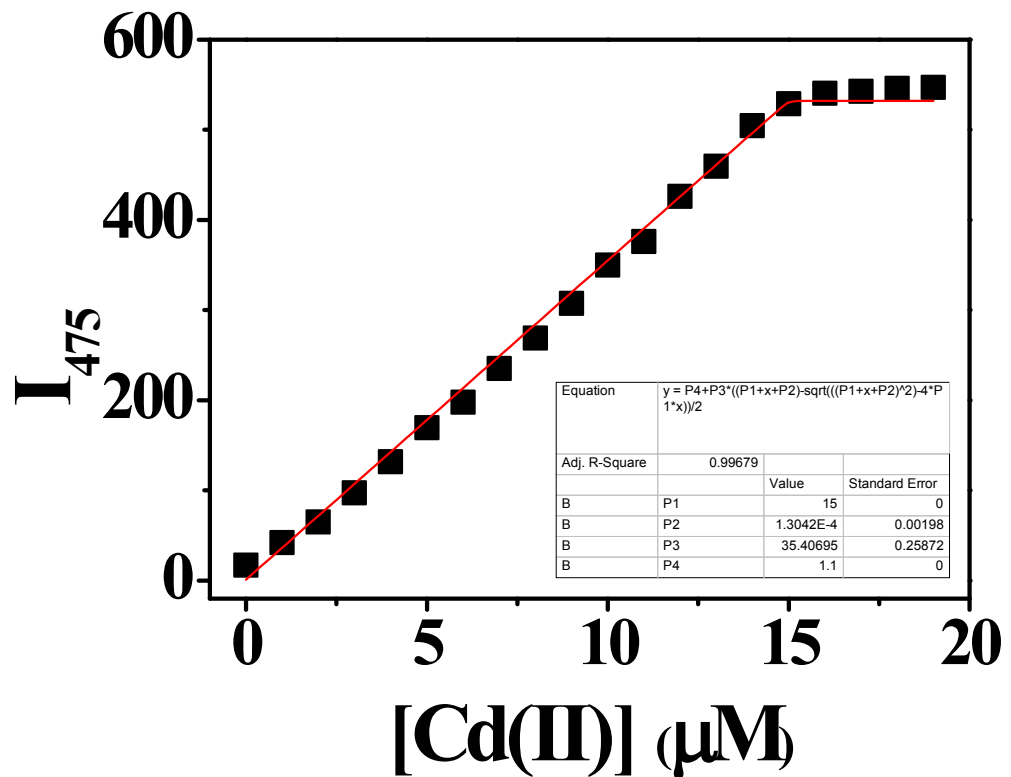


Figure S11. Non-linear least square fitting of the emission intensity of **1** ($15 \mu M$) as a function of concentration of Cd^{2+} by a 1:1 complex model.

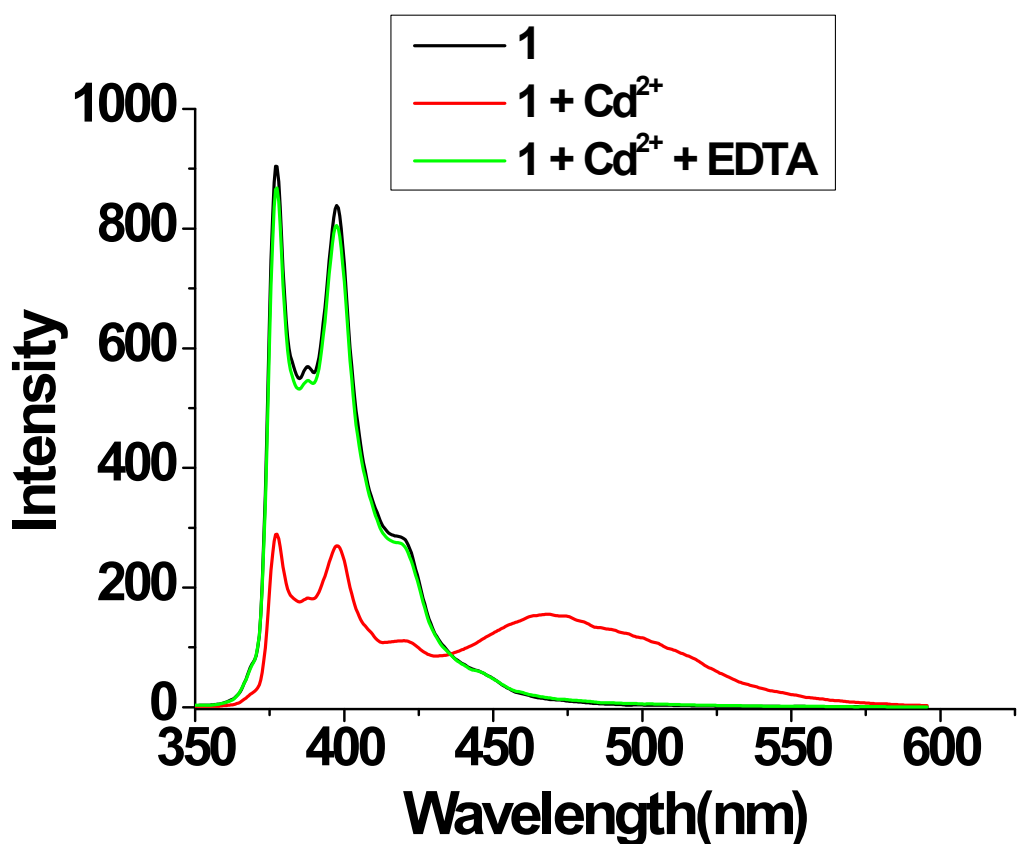


Figure S12. Fluorescence emission spectra of **1** (10 μ M) in the absence and presence of Cd²⁺ (1 equiv) and EDTA (1 equiv) in aqueous buffered solutions (10 mM, HEPES, pH 7.4) containing 1% DMF ($\lambda_{\text{ex}} = 342$ nm).

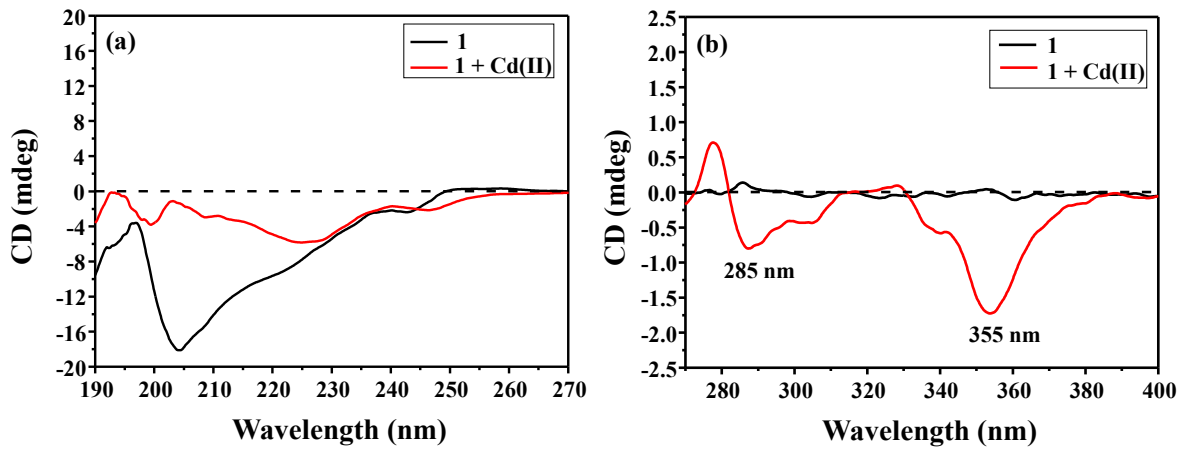


Figure S13. (a) Far- and (b) Near-UV CD Spectra of **1** (75 μM) in the absence or presence of Cd^{2+} (75 μM) in aqueous buffered solutions (10 mM PBS, pH 7.4) containing 5% (v/v) 2,2,2-trifluoroethanol.

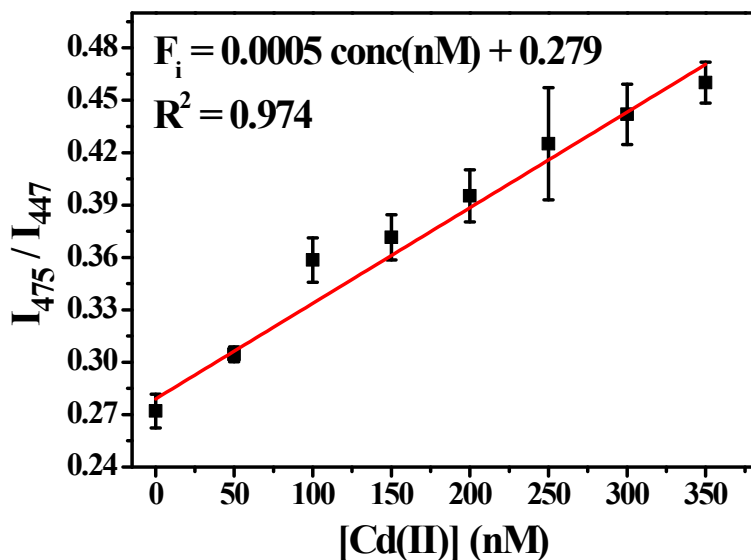


Figure S14. Linear curve fitting of emission intensity ratio change of **1** (15 μM) as a function of the concentration of Cd^{2+} in aqueous buffered solutions (10 mM, HEPES, pH 7.4) containing urine samples.

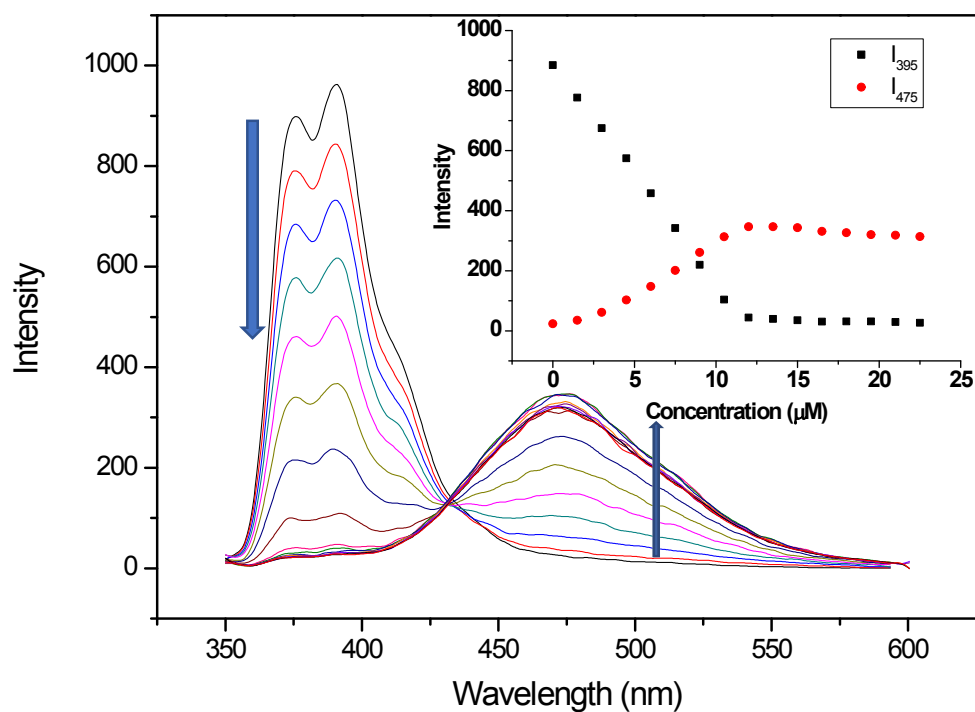


Figure S15. Emission spectra of **1** (15 μM) with increasing concentration of Cd²⁺ in aqueous buffered solutions (10 mM HEPES, pH 7.4) containing ground waters.

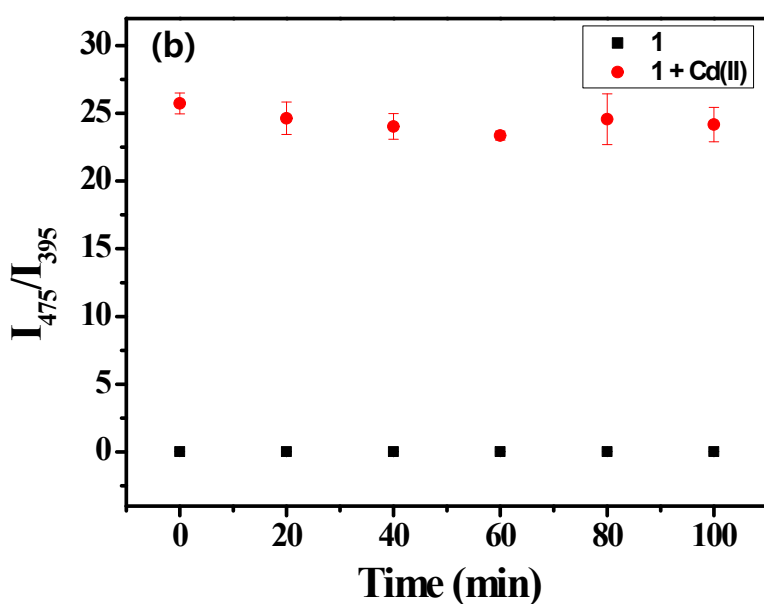
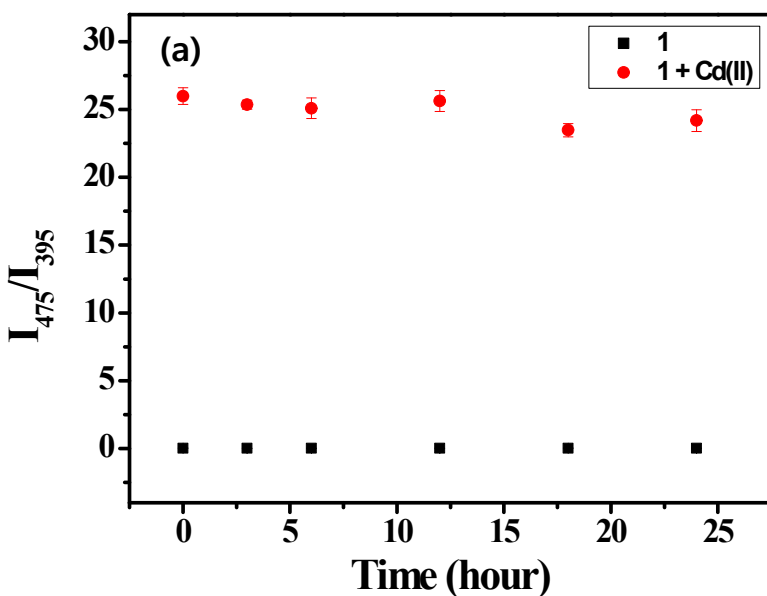


Figure S16. (a) Incubation of stock solution of **1** at room temperature for 24 hrs and emission intensity ratio of **1** (15 μ M) by Cd^{2+} (15 μ M) (b) Upon addition of Cd^{2+} into the solution containing **1**, emission intensity ratio induced by Cd^{2+} for 100 mins in aqueous buffered solutions (10 mM, HEPES, pH 7.4) containing 1% DMF.

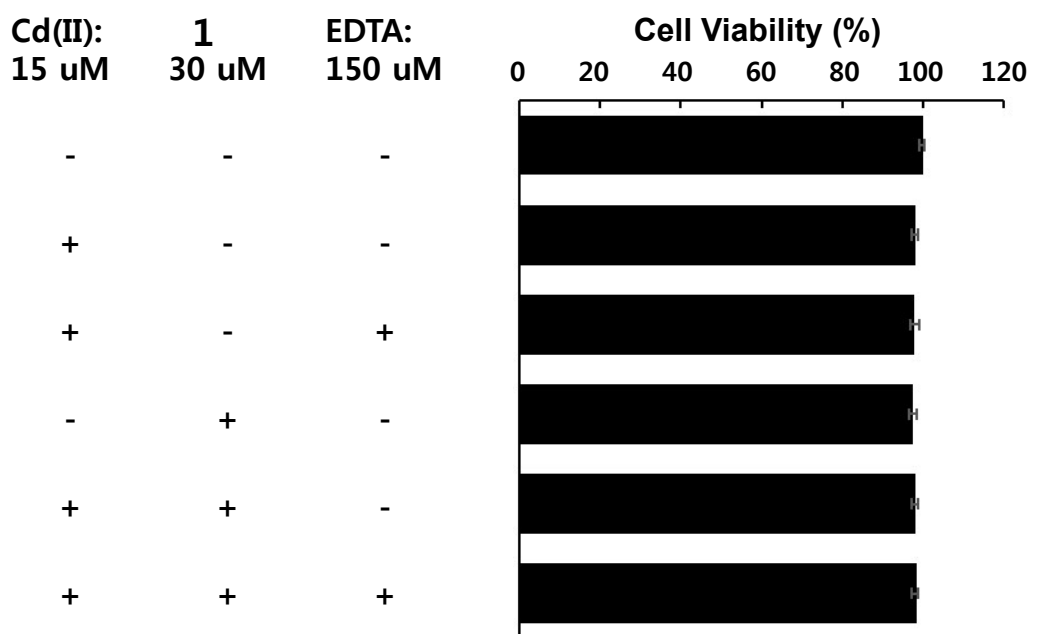


Figure S17. MTS assay for the viability of MDA-MB-231 cells in DMEM 10% FBS treated with **1**, **1** + Cd(ClO₄)₂, and **1** + Cd(ClO₄)₂ + EDTA for 24 h.

Table S1 Comparison of the properties of ratiometric fluorescent probes for Cd(II) in aqueous solution.¹⁻¹¹

| Fluorophore(s) | Organic cosolvent | Emission bands (nm) | Change (fold) | LOD | Response | Application |
|---|-------------------|---------------------|-----------------|-----------------|--|-------------------|
| Dansyl Trp | 0% | 350 to 500 | 9 | 0.9 μM | Hg(II), Zn(II), Ag(I) | No cell image |
| Dansyl Trp | 0% | 350 to 500 | 4 | 0.3 μM | Cu(II), Zn(II) | No cell image |
| 5-Dimethylamino-2-(2-pyridinyl)-benzoimidazole | 0% | 493 to 587 | 8 | 0.3 pM | Zn(II) | Cell image |
| Coumarin | 0% | 328 to 368 | 3.5 | 40 pM | Zn(II) | Cell image |
| 4,5-Diamino-1,8-naphthalimide | 10% EtOH | 487 to 531 | 3 | 0.1 μM | Zn(II) | No cell image |
| Boradiazaindacene (BODIPY) | 90% Acetone | 550 to 800 | 13 | ND ^a | Cr(III), Ni(II), Cu(II) | Cell image |
| 8-Hydroxyquinoline norbornene | 50% Methanol | 330 to 600 | 2 | 1.6 nM | Zn(II) | Paper strip |
| 8-Hydroxyquinoline | 80% Ethanol | 350 to 650 | 4.5 | 23.6 nM | Zn(II) | Cell image |
| 8-Hydroxy-2-methyl quinoline | 80% Dioxane | 400 to 700 | 92 | 20 nM | Cu(II), Zn(II) | No cell image |
| 4-Isobutoxy-6-(dimethylamino)-8-methoxyquinaldine | 0% | 400 to 700 | 3 | 9.6 pM | Mn(II), Fe(II), Co(II), Ni(II), Cu(II), Hg(II), Pb(II), Zn(II) | Cell image |
| Phenanthro[9,10-d]oxazole | 50% DMF | 400 to 600 | ND ^a | ND ^a | Fe(III), Hg(II), Pb(II), Cu(II) | Paper strip |
| Pyrene (Present work) | 1% DMF | 395 to 475 | 28 | 22 nM | Only Cd(II) | Cell image, Urine |

^aND means not determined.

References

- 1 B. P. Joshi, J. Park, W. I. Lee, K. H. Lee, *Talanta.*, 2009, **78**, 903–909.
- 2 Y. Li, L. Li, X. Pu, G. Ma, E. Wang, J. Kong, Z. Liu, Y. Liu, *Bioorg. Med. Chem. Lett.*, 2012, **22**, 4014–4017.
- 3 Z. Liu, C. Zhang, W. He, Z. Yang, X. Gao, Z. Guo, *Chem. Commun.*, 2010, **46**, 6138–6140.
- 4 M. Taki, M. Desaki, A. Ojida, S. Iyoshi, T. Hirayama, I. Hamachi, Y. Yamamoto, *J. Am. Chem. Soc.*, 2008, **130**, 12564–12565.
- 5 C. Lu, Z. Xu, J. Cui, R. Zhang, X. Qian, *J. Org. Chem.*, 2007, **72**, 3554–3557.
- 6 X. Peng, J. Du, J. Fan, J. Wang, Y. Wu, J. Zhao, S. Sun, T. Xu, *J. Am. Chem. Soc.*, 2007, **129**, 1500–1501.
- 7 S. Sarkar, R. Shunmugam, *ACS Appl. Mater. Interfaces.*, 2013, **5**, 7379–7383.
- 8 Z. Shi, Q. Han, L. Yang, H. Yang, X. Tang, W. Dou, Z. Li, Y. Zhang, Y. Shao, L. Guan, W. Liu, *Chem. Eur. J.*, 2015, **21**, 290–297.
- 9 Y. Bao, B. L. Liu, H. Wang, F. Du, R. Bai, *Anal. Methods.*, 2011, **3**, 1274–1276.
- 10 L. Xue, G. Li, Q. Liu, H. Wang, C. Liu, X. Ding, S. He, H. Jiang, *Inorg. Chem.*, 2011, **50**, 3680–3690.
- 11 L. Ahang, Q. Tong, L. Shi, *Dalton Trans.*, 2013, **42**, 8567–8570.